J. Agr. Sci. Tech. (2015) Vol. 17: 589-600

Determination of Cherry Color Parameters during Ripening by Artificial Neural Network Assisted Image Processing Technique

S. Taghadomi-Saberi[1], M. Omid[1*], Z. Emam-Djomeh[2], and Kh. Faraji-Mahyari[1]

ABSTRACT

Among the different classes of physical properties of foods, color is considered the most important visual attribute in quality perception. Consumers tend to associate color with quality due to its good correlation with physical, chemical and sensorial evaluations of food quality. This study used an inexpensive method to predict sweet cherries color parameters by combining image processing and artificial neural network (ANN) techniques. The color measuring technique consisted of a CCD camera for image acquisition, MATLAB software for image analysis, and ANN for modeling. To demonstrate the usefulness of this technique, changes of cherry color during ripening were studied. After designing, training, and generalizing several ANNs using Levenberg-Marquardt algorithm, a network with 7-14-11-3 architecture showed the best correlation (R^2= 0.9999) for *L, *a** and *b** values from Chroma meter and the machine vision system. *L** and *b** parameters decreased during ripening of cherries and *a** parameter increased at first and then decreased. Evaluation of *L**, *a** and *b** values showed the possibility of reliable use of this system for determination of absolute color values of foodstuffs with a much lower cost in comparison with Chroma meter.**

Keywords: Cherry fruit, Color parameters *L*, *a* and *b*, Modeling.

INTRODUCTION

Iran is the third largest producer of sweet cherry *(Prunusavium)* in the world, after Turkey and United States of America (Anon., 2010). The changes in cherry (Takdaneh variety) color during ripening is shown in Figure 1. The senescence period changes in 6 stages, from green to yellow, pink, light red, red, and finally to black.

Consumers select their foods primarily based on visual perception which is a mix of the color, shape, and size of the product. Among the different classes of physical properties of foods and foodstuffs, color is considered the most important visual attribute in the perception of product quality and consumers tend to associate color with flavor, safety, storage time, nutrition, and level of satisfaction due to the fact that it correlates well with physical, chemical, and sensorial evaluations of food quality (Pedreschi *et al*., 2006; Valadez-Blanco *et al*., 2007; Iqbal *et al*., 2010). In image analysis for food products, color is an influential attribute and powerful descriptor that often implies object extraction and identification and it can be used to quantify the color distribution of non-homogeneous samples (Brosnan and Sun, 2003).

Three frequently used color approaches include RGB, HSV, and CIELab color spaces. Red, green, and blue (RGB) color

[1] Department of Agricultural Machinery Engineering, Faculty of Agricultural Engineering and Technology, University of Tehran, Karaj, Islamic Republic of Iran.
*Corresponding author; e-mail: omid@ut.ac.ir
2 Department of Food Sciences and Technology, Faculty of Agricultural Engineering and Technology, University of Tehran, Karaj, Islamic Republic of Iran.

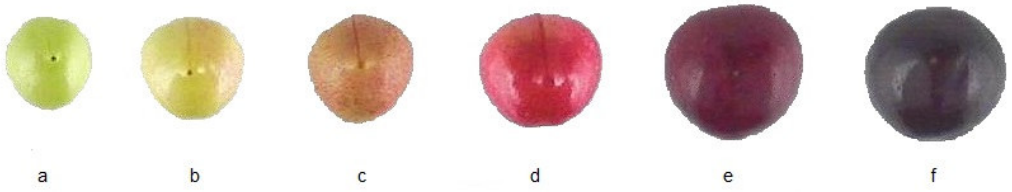

Figure 1. Sweet cherry ripeness stages.

space can describe over 16 million colors by combining different amounts of red, green, and blue, with possible values ranging from 0 to 255. Although the RGB method is capable of distinguishing between millions of colors, it is not representative of how humans perceive color. The second approach is hue, saturation, and value (HSV) color space, in which values range from 0 to 1.0 for each of the 3 variables. As hue moves from 0 to 1.0, color varies from red, yellow, green, cyan, blue, magenta, and then back to red. Saturation values vary from 0 to 1.0, increasing with the amount of black in the color. Value represents the brightness of the colors specified by hue and colors become increasingly brighter as value varies from 0 to 1.0. HSV values can also be represented as values ranging from 0 to 255, making it easier to transform between the RGB and HSV color representations. The HSV color space better represents how humans perceive color, due to the varying levels of saturation and value (Zhou *et al*., 2004). The third approach uses *CIE Lab* color space. CIE is often used in food research studies. The *L*a*b** color space is device independent, providing consistent color regardless of the input or output devices such as digital camera, scanner, monitor and printer (Yam and Papadakis, 2004). The CIE standard Lab color spaces experiments have revealed that the *L*, a** and *b** values are easier to be related to the perceived color than other existing scales. This color space (L*a*b*) is often used in food research studies and almost always the color of foods has been measured in *L*a*b** mode. Food color information could be accomplished using commercial software packages such as Photoshop or MATLAB (Afshari-Jouybari and Farahnaky, 2011). Such software not only can be applied to simulate the role of available commercial colorimetric instruments with much lower cost, but are also more accessible nowadays. In other words, the advantages of this method including its acceptable accuracy, simplicity, availability, and low cost, make it more practical.

Machine vision (MV) is a technique for acquiring and analyzing an image of a real scene by computers for obtaining information or controlling processes (Brosnan and Sun, 2003). The use of MV for the quality inspection of fruits and vegetables has increased during recent years (Blasco *et al*., 2003). Quality evaluation, detection of defects, identification, grading and sorting of fruits and vegetables, meat and fish, bakery products, and prepared goods, among others, are the examples of MV in the food industry (Yoshida *et al*., 2008; Omid *et al*., 2010a; Unay *et al*., 2011). For instance, Kılıç *et al*. (2007) developed a computerized inspection system to determine food *L*a*b** and found a good agreement, i.e. R^2 of 0.958, 0.938, and 0.962 for *L*, a**, and *b**, respectively, between color measurement with computerized inspection system and a spectrophotometer. Afshari-Jouybari and Farahnaky (2011) studied the potential of using digital imaging and Photoshop software and Artificial Neural Network (ANN) for measurement of Mazafati date fruit color change during accelerated ripening, compared to the Hunter Lab system. The correlation

coefficient obtained between Photoshop and Hunter Lab was 0.991, 0.966, and 0.987 for *L*, a** and *b** values, respectively. Recently, Behroozi Khazaei *et al*. (2103) implemented a MV system to evaluate grape drying through an assessment of the fruit's shrinkage and quality during the dehydration. Anthocyanin content constantly increased during ripening stages of sweet cherry as color changed from green to red as seen in Figure 1 (Taghadomi-Saberi *et al*., 2013). Anthocyanin, which is a pigment, is well correlated with color of cherry; therefore, anthocyanin and color can both be considered as a good discriminant for cherry ripening. Generally, the use of MV for color quality estimation requires an absolute color calibration technique based on a common interchange format for color data and a knowledge of which features from an image can be best correlated with product quality. Rapid advances in hardware and software for digital image processing (DIP) have led to several studies on the development of MVs (Brosnan and Sun, 2003).

Various techniques such as ANN, statistical learning (SL), fuzzy logic (FL) and genetic algorithm (GA) have been applied increasingly for agri-food quality evaluation using MV in recent years (Du and Sun, 2006; Abbasgholipour *et al*., 2011; Fadilah *et al*., 2012). ANNs are composed of interconnecting artificial neurons (programming constructs that mimic the properties of biological neurons). ANNs may either be used to gain an understanding of biological neural networks, or for solving artificial intelligence problems without necessarily creating a model of a real biological system. The real biological nervous system is highly complex; ANN algorithms attempt to abstract this complexity and focus on what may hypothetically matter most from an information processing point of view. Du and Sun (2006) reviewed latest advances in learning techniques such as ANNs, SL, FL and GA for food quality evaluation using MV. Abbasgholipour *et al*. (2011) implemented a supervised color image segmentation using a permutation-coded GA to identify regions in hue–saturation–intensity (HSI) color space for desired and undesired raisin detection in various conditions. There are a large number of researches applying ANN for food-related topics. For instance, by using DIP and ANN, Fadilah *et al*. (2012) classified ripeness stages of oil palm fresh fruit bunch based on color features. They could improve classification accuracy from 91.67 to 93.33% by applying principal component analysis (PCA). In another work, Momenzade *et al*. (2012) applied ANN for predicting drying time of green pea in a microwave assisted fluidized bed dryer. Error analysis results revealed that a network with the 'Log sigmoid' transfer function and "trainrp" back propagation algorithm was the most appropriate ANN model for predicting drying time of green pea.

Unlike commercial Chroma meters which measure only a small area, MV systems can be more useful for food color analysis. Although it is possible to convert from RGB to *L*a*b** in "Image processing' toolbox of MATLAB", it cannot determine the exact values of *L*a*b** and it can only be useful to study the *L*a*b** color parameter changes during a process. As mentioned above, ANN is a powerful artificial intelligence technique and a back propagation ANN with weights, biases, a sigmoid layer, and a linear output layer are capable of approximating any function with a finite number of discontinuities (Wu and Chan, 2009). In this study, an intelligent system based on MV and ANN was implemented for determining *L*, a** and *b** color parameters of sweet cherries during ripening of the fruit. The ripeness stages of cherry were used as a case study due to having different colors. Furthermore, cherry ripeness stages are important from physiochemical point of view. Antioxidant activity and phenolic compounds, possibly correlated with color changes, vary constantly during ripening of cherry, therefore, determination of cherry

ripeness stages can be very useful (Taghadomi-Saberi *et al*., 2013).

MATERIALS AND METHODS

Samples Preparation

Takdaneh cherry samples were obtained from a field located in Shahrestanak, Alborz, Iran and transported to the Agricultural Machinery Department, University of Tehran. The fruits were stored in a refrigerator after detaching their stems. Fruits in different ripeness stages were chosen by visual inspection and color chart (Figure 1). Based on visual inspection (color and size), a panel of researchers separated fruits into ripeness stages (Polder *et al*., 2003; Serrano *et al*., 2005; Fu *et al*., 2011; Taghadomi-Saberi *et al*., 2013). More specifically, these stages coincided with 12, 10, 9, 7, and 7 days intervals from each other.

Color Measurement

The color measurement setup consisted of CCD camera (PROLINE UK, Model 565s with 510 by 492 pixel resolutions, London, United Kingdom), capture card (WinFast DV2000 with a 320Hx240V resolution), 2 fluorescent tubes around camera as lighting system providing uniform light and eliminating shadow images of fruits, and a personal computer. The camera was mounted 10 cm above the white background (white color has good and acceptable contrast with cherries) and powered by a 24V power supply. The light source and camera were mounted on a frame and were attached to the measurement table. The whole system was covered by a tarpaulin to omit the effects of surrounding lights. Captured signals by the camera were transferred to the computer through the video capture card, digitized and stored on the computer into RGB coordinates for further analysis (Omid *et al*., 2010a) (Figure 2).

Using the aforementioned setup, images of sweet cherries were taken and their color values were measured by a KONICA MINOLTA CR-403 Chroma meter made in Japan. To assess the system performance in different ranges of colors, 12 colored cards were used with different colors proportional to cherry colors during ripeness period (Figure 3). True color values of each card were measured by means of Chroma meter, then, image of each card was taken with our setup for calibration purposes.

Cherry Fruit Segmentation

When the fruit is well contrasted against the background, fruit localization could be undertaken by classical supervised or

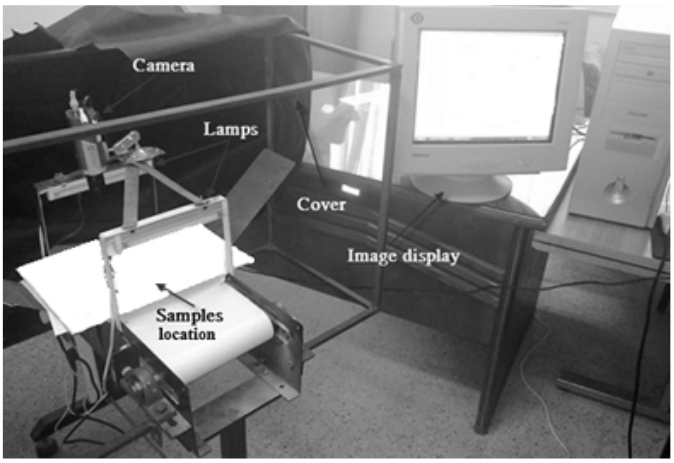

Figure 2. The machine vision system.

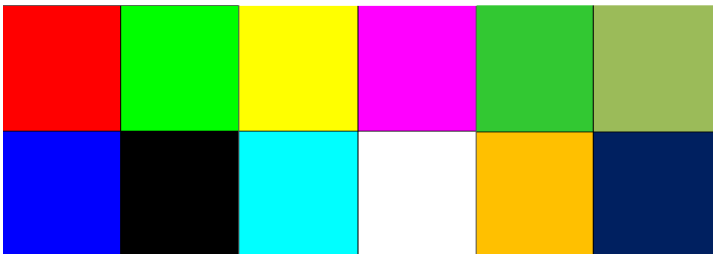

Figure 3. Colored cards for calibration.

unsupervised threshold techniques (Fu *et al*., 2011). The fruit area was segmented from the background with the thresholding and the Otsu's algorithm techniques (Otsu, 1979). The saturation parameter, *S* in HSV color space, was very effective in segmenting the cherry from the background, although being a non-linear combination of the red, green, and blue values, it required more computation. It was found that a simple thresholding was not enough because of different colors of cherries in different ripeness stages and, possibly, because of noises due to shadows. Accordingly, different thresholding values were used at different stages. The thresholding value for each stage was chosen based on the average of R and G channels of cherry images (Table 1).

Conversion of RGB Color Values to *L**, *a** and *b**

The result of segmentation was an image containing one cherry. From each cherry, a set of features was extracted to describe the sample. In image processing problems, many different features have been developed and used. The feature analyses of cherry include extraction of color features. In this study, 37 features common in this field were extracted and applied (Venora *et al*., 2009; Mollazade *et al*., 2012). These applied features are listed in Table 2.

In order to improve the performance of the system and have a sufficient feature vector, it seemed necessary to find a way for reducing the dimension of the input vector and discarding unimportant data from the feature vector and therewith accelerate the process. An effective procedure to reduce the dimension of the input vector is using PCA (Omid *et al*., 2010b). Accordingly, the resulting data were subjected to PCA. We used MATLAB software and assigned 0.02 to maximum fraction of variance for removed rows. PCA processes matrices using principal component analysis so that each row is uncorrelated; the rows are in the order of the amount they contribute to total variation. The rows whose contribution to total variation was less than maximum fraction (0.02) were removed. After PCA process, seven PCs were selected, i.e. RGB attributes abstracted into seven elements. This means that by using PCA, a 77.42% reduction in input volume was achieved.

Table 1. The thresholding value for each stage based on the average of R and G channels of cherry image.

Condition	Threshold value	Stages
Mean R^a> 206	S^a> 0.2 and H^a< 0.2	4
190< Mean_*R*< 206 and Mean_G^a> 195	S> 0.13	3 , 4
190< Mean_*R*< 206 and Mean_*G*< 195	S> 0.25	2 , 3
180< Mean_*R*<190 and Mean_*G*< 190	S> 0.3	2 , 6
Otherwise	V^a< 0.62	1 , 5

[a] *R* and *G* are the first and second channels of RGB images, respectively. *H, S* and *V* are the first, second and third channels of HSV images, respectively.

Table 2. Available features measured by image analysis for each cherry.

F_ no	Features		
1-3	$r\_m = Mean(R^a)$	$g\_m = Mean(G^a)$	$b\_m = Mean(B^a)$
4-6	$t_1 = \frac{R}{R+G+B}$	$t_2 = \frac{G}{R+G+B}$	$t_3 = \frac{B}{R+G+B}$
7-9	$r\_g = R - G$	$r\_b = R - B$	$b\_g = B-G$
10-12	$v\_r = Var(R)$	$v\_g = Var(G)$	$v\_b = Var(B)$
13-15	$Skew\_r = Skewness(R)$	$Skew\_g = Skewness(G)$	$Skew\_b = Skewness(B)$
16-18	$Kor\_r = Kurtosis(R)$	$Kor\_g = Kurtosis(G)$	$Kor\_b = Kurtosis(B)$
19-21	$m\_r\_g = Mean(r\_g)$	$m\_r\_b = Mean(r\_b)$	$m\_b\_g = Mean(b\_g)$
22-24	$v\_r\_g = Var(r\_g)$	$v\_r\_b = Var(r\_b)$	$v\_b\_g = Var(b\_g)$
25-27	$Skew\_r\_g = Skewness(r\_g)$	$Skew\_r\_b = Skewness(r\_b)$	$Skew\_b\_g = Skewness(b\_g)$
28-30	$Kor\_r\_g = Kurtosis(r\_g)$	$Kor\_r\_b = Kurtosis(r\_b)$	$Kor\_b\_g = Kurtosis(b\_g)$
31-33	$Skew\_t_1 = Skewness(t_1)$,	$Skew\_t_2 = Skewness(t_2)$	$Skew\_t_3 = Skewness(t_3)$
34-36	$Kor\_t_1 = Kurtosis(t_1)$,	$Kor\_t_2 = Kurtosis(t_2)$	$Kor\_t_3 = Kurtosis(t_3)$
37	The number of pixels		

[a] *R, G* and *B* are the first, second and third channels of RGB images, respectively.

These features were then fed to ANN models as input vector.

Artificial Neural Networks Modeling

In this research, ANN as implemented in MATLAB was used for modeling the relationship between *L*a*b** values measured by means of the Chroma meter and color characteristics extracted from the images of cherries. Levenberg-Marquardt (LM) algorithm and "trainbr" function was used to train the networks. The "trainbr" is a network training function that updates the weight and bias values according to LM optimization. It minimizes a combination of squared errors and weights, and then determines the correct combination so as to produce a network that generalizes well. The process is called Bayesian Regularization (BR), hence the name "trainbr" to describe this process.

Image analysis routines were integrated into a software programmed in MATLAB that converted the RGB color of the cherry images into *L*a*b** units. In this way, the color of cherries could be calculated in *L*a*b** units over the whole fruit pixels shown in the images.

To evaluate the performance of ANN, the *L*, a** and *b** parameters were determined by use of MATLAB command for conversion from RGB to *L*a*b** color space.

Accuracy Assessment and Calibration

Three widely used statistical parameters (Taghadomi-Saberi *et al*., 2013) including mean absolute error [MAE, Equation (1)], mean square error [MSE, Equation (2)], and mean absolute percentage error [MAPE, Equation (3)] were used for measurement of accuracy and differences between the values achieved by MV setup (y_0) and the actual color values (y_p) achieved by Chroma meter for '*n*' samples:

$$MAE_y = \frac{\sum_{i=1}^{n} |y_O - y_P|}{n} \quad (1)$$

$$MSE_y = \frac{\sum_{i=1}^{n} (y_O - y_P)^2}{n} \quad (2)$$

$$MAPE_y = \frac{\sum_{i=1}^{n}\left(\frac{|y_O - y_P|}{y_O}\right)}{n} \times 100 \quad \% \qquad (3)$$

RESULTS AND DISCUSSION

At first, data were divided into two categories: 31 samples (approximately 89%) for training and four samples (approximately 11%) for testing. To have better results, the data were initially normalized. In order to normalize the data, the mean was mapped to zero and deviation to one. Several ANNs were designed, trained, and generalized using the MATLAB Neural network Toolbox. A back propagation network with weights, biases, a sigmoid layer, and a linear output layer are capable of approximating any function with a finite number of discontinuities (Wu and Chan, 2009). Thus, back propagation algorithm was chosen to build the prediction models. The results of trial and error showed that two-hidden layer models were generally better than the others, so these networks were considered further. The results obtained from the six models having one or two hidden layers and their characteristics are illustrated in Table 3. Among these, the best performance, without overtraining, was achieved with a back propagation neural network that used "trainbr" as training function and with 14 neurons in the first hidden layer and 11 in the second one, with both layers using "hyperbolic tangent sigmoid" as their transfer function (Figure 4). This two-hidden-layer network has 7-14-11-3 architecture, i.e. the best model consisted of an input layer with seven input variables (7 PCs), two hidden layers with 14 and 11 neurons in each layer, and an output layer with three output variables (L*, a* and b*), highlighted in Table 3. This architecture has the lowest values of *MSE, MAE* and *MAPE* for all output variables indicating that the ANN predicting *L*a*b** values by this model tend to follow the corresponding actual ones quite closely (Table 3).

Table 3. Performance of Neural networks results related to *L*, a** and *b*.*[a]

Color p.	N_{H1}	N_{H2}	MSE	MAE	MAPE (%)	R^2
L*	10	-	0.1030	0.1955	0.0044	0.9996
	11	-	0.0356	0.1313	0.0031	0.9999
	11	12	0.0252	0.1003	0.0023	0.9999
	12	8	0.0420	0.1287	0.0030	0.9998
	13	8	0.0014	0.0250	0.0006	0.9999
	14	**11**	**0.0006**	**0.0177**	**0.0004**	**0.9999**
a*	10	-	0.0460	0.1612	0.0136	0.9999
	11	-	0.0297	0.1341	0.0074	0.9999
	11	12	0.0340	0.1560	0.0113	0.9999
	12	8	0.0268	0.1233	0.0073	0.9999
	13	8	0.0023	0.0343	0.0021	0.9999
	14	**11**	**0.0015**	**0.0258**	**0.0013**	**0.9999**
b*	10	-	0.0265	0.1205	0.0101	0.9999
	11	-	0.0213	0.1070	0.0125	0.9999
	11	12	0.0135	0.0850	0.0086	0.9999
	12	8	0.0161	0.0849	0.0073	0.9999
	13	8	0.00082	0.0232	0.0027	0.9999
	14	**11**	**0.0005**	**0.0165**	**0.0024**	**0.9999**

[a] N_{Hi} is the number of neurons in the *i*th hidden layer. *MSE, MAE, MAPE* and R^2 stand for mean square error, mean absolute error, mean absolute percentage error and coefficient of determination, respectively.

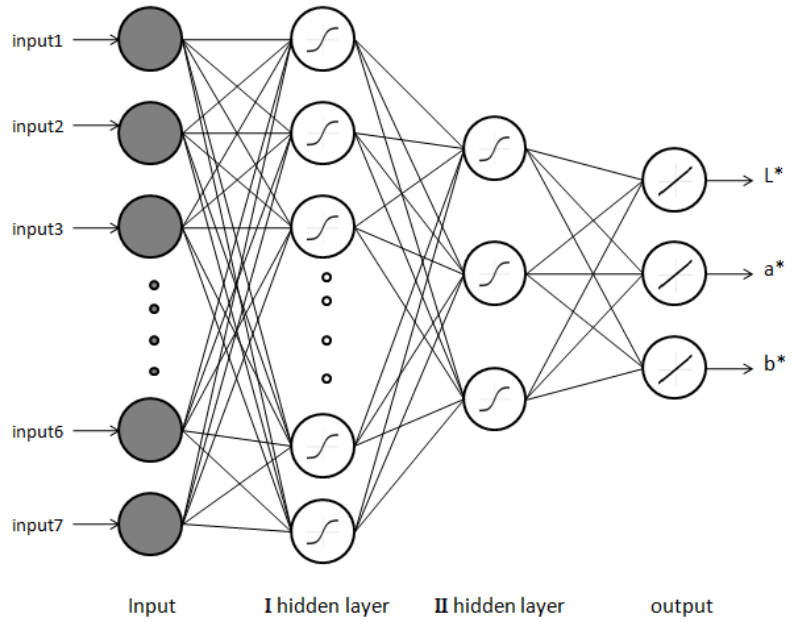

Figure 4. Architecture of the artificial neural network used.

Therefore, this model (7-14-11-3) was selected as the best solution for determination of the color parameters. The obtained determination coefficient of values related to "RGB to *L*a*b**" conversion command (R^2= 0.748) in MATLAB image processing toolbox showed that this command could not be reliable for determining the absolute values of *L*a*b** parameters, and maybe just suitable for representing the changes of color parameters during a procedure.

The determination coefficients between modeled and Chroma meter color parameters were 0.9999 for *L**, *a** and *b** values (Figure 5). Evaluation using digital imaging and Photoshop software for measurement of Mazafati date fruit color parameters yielded 0.991, 0.966 and 0.987 as correlation coefficients for *L**, *a** and *b** values, respectively. Modifying the results of Photoshop, Afshari-Jouybari and Farahnaky (2011) applied five calibration methods including linear equation, polynomial equation, linear model, quadratic model, and ANN. They concluded that ANN was the most resilient method among others to follow the real values of color parameters. In comparison with previous researches on determining these color parameters (Kılıç *et al*., 2007; Afshari-Jouybari and Farahnaky, 2011), the results of the present study show that using two-hidden-layers ANN and MATLAB software is remarkably easier than Photoshop for image processing, and even a better improvement can be achieved. ANN is more reliable in comparison with not only the basic modifiers such as polynomial equation, but also the advanced techniques such as ANFIS in some cases. Taghadomi-Saberi *et al*. (2014) concluded that ANN outperformed ANFIS for estimating antioxidant activity and anthocyanin content of sweet cherry. Mollazade *et al*. (2012) applied four different data mining (DM) techniques, among which a 7-6-4 ANN had the highest correlation coefficient for grading raisins. There also exists a wide range of successful applications of various DM techniques, especially ANNs, in the food industry. Generally, our system can be used for determination of color parameters at a wide range of *L**, *a** and *b** and it can simulate

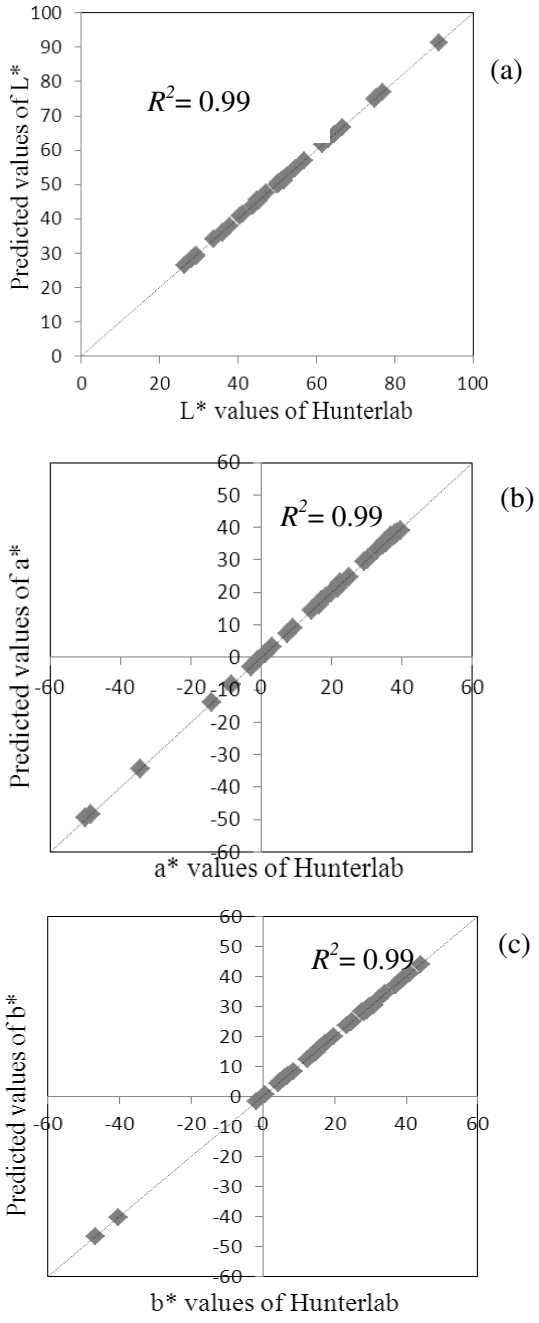

Figure 5. Correlation between *L** (a), *a** (b) and *b** (c) values of Chroma meter and predicted values.

Chroma meter performance well with a very low cost CCD camera.

Color parameters changes of cherry fruits during ripening are presented in Figure 6. *L** and *b** parameters decreased during ripeness of cherries and *a** increased at first (up to stage "c") and then decreased. Serrano *et al.* (2005) reported similar results for evolution of fruit skin color parameters (L*, a*, and b*) over the developmental stages of sweet cherry. Physiologically, at red stage, cherry fruit is mature and reaches its maximum weight and size. At stage "d", fruit ripening starts, its color changes from red to black and its texture becomes soft. Many reports have been published on the loss of fruit firmness during ripening. They chiefly concern changes in cell wall components and their enzymatic breakdown (Huber, 1983). The appearance, during ripening, of pectolytic enzymes, such as pectinesterase and polygalacturonase, is often related to softening (Fils-Lycaon and Buret, 1990). As firmness decreases during maturity, pectin content increases. Actually, the pectins soluble in water (WSP) and in oxalate (OSP) increase, while those soluble in hydrochloric acid (HSP) decrease.

CONCLUSIONS

In this study, the color parameters *L*, a** and *b** of sweet cherries were determined by use of ANN assisted MV system under controlled conditions (illumination, distance between camera and objects, including cherries and color cards, camera angle, and light source) using MATLAB software. By using thresholding technique and Otsu's algorithm, the cherries at different stages of ripeness were segmented successfully. ANN with 7-14-11-3 architecture had the best results (R^2= 0.9999) for modeling *L*a*b** color parameters of sweet cherry during ripening process. Evaluation of Chroma meter and modeled *L*a*b** values showed that this system could be used for determination of absolute color values for food materials. Accuracy of this system was comparable with the available commercial colorimetric instruments. However, low cost of this system makes it more useful.

The color measuring technique discussed in this study consisted of a CCD camera for image acquisition, fluorescent illuminants,

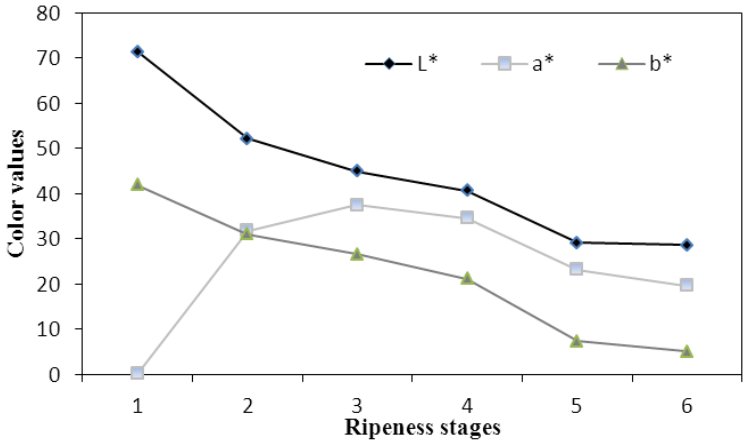

Figure 6. Color parameter changes during ripeness stages.

capture card and MATLAB software for image analysis and has been used to provide a more versatile way to measure the color of many foods more than the traditional expensive color-measuring instruments. Overall, the method presented in this study can be extended for evaluating *L*a*b** in food colorimetry. By using this model and previous researches on the chemical content of cherries during ripening (e.g., anthocyanin content), extracting chemical features without destructive experiment is possible.

ACKNOWLEDGEMENTS

The financial support provided by the University of Tehran, Iran, is gratefully acknowledged.

REFERENCES

1. Abbasgholipour, M., Omid, M., Keyhani, A. R. and Mohtasebi, S. S. 2011. Color Image Segmentation with Genetic Algorithm in a Raisin Sorting System Based on Machine Vision in Variable Conditions. *Expert Syst. Appl.,* **38:** 3671–3678.
2. Afshari-Jouybari, H. and Farahnaky, A. 2011.Evaluation Photoshop Software Potential for Food Colorimetry. *J. Food Eng.,* **106:** 170–175.
3. Anonymous. 2010. Countries by Commodity: 2010. *Food and Agriculture Organization of the United Nations.* FAOSTAT, 2 October 2012, Available at: www.faostat.fao.org.
4. Behroozi Khazaei, N., Tavakoli Hashjin, T., Ghassemian, H., Khoshtaghaza, M. H. and Banakar, A. 2013. Application of Machine Vision in Modeling of Grape Drying Process. *J. Agr. Sci. Tech.,* **15:** 1095-1106.
5. Blasco, J., Aleixos, N. and Molto, E. 2003. Machine Vision System for Automatic Quality Grading Fruit. *Biosyst. Eng.,* **85:** 415–423.
6. Brosnan, T. and Sun, D. W. 2003. Improving Quality Inspection Food Products by Computer Vision: A Review. *J. Food Eng.,* **61**: 3–16.
7. Du, C. J. and Sun, D. W. 2006. Learning Techniques Used in Computer Vision for Food Quality Evaluation: A Review. *J. Food Eng.,* **72:** 39–55.
8. Fadilah, N., Mohamad-Saleh, J., Abdul Halim, Z., Ibrahim, H. and Syed Ali, S.S. 2012. Intelligent Color Vision System for Ripeness Classification of Oil Palm Fresh Fruit Bunch. *Sensors.* **12**: 14179-14195.
9. Fils-Lycaon, B. and Buret, M. 1990. Loss Firmness and Changes in Pectic Fractions during Ripening and Over-ripening of Sweet Cherry. *J. Am. Soc. Hortic. Sci.,* **25:** 777-778.
10. Fu, L., Okamoto, H., Kataoka, T. and Shibata, Y. 2011.Colorbased Classification

for Berries Japanese Blue Honeysuckle. *Int. J. Food Eng.,* **7**: 1-12.

11. Huber, D. J. 1983. The Role Cell Wall Hydrolyses in Fruit Softening. *Hortic. Rev.,* **5**: 169–219.
12. Iqbal, A., Valous, N. A., Mendoza, F., Sun, D. W. and Allen, P. 2010. Classification Presliced Pork and Turkey Ham Qualities Based on Image Color and Textural Features and Their Relationships with Consumer Responses. *Meat Sci.*, **84:** 455–465.
13. Kılıç, K., Onal-Ulusoy, B., Yıldırım, M. and Boyacı, I. H. 2007. Scanner-based Color Measurement in Lab Format with Artificial Neural Networks (ANN). *Eur. Food Res. Technol.,* **226:** 121–126.
14. MATLAB R2009a, Matlab user's guide. The MathWorks Inc., Massachusetts, USA: Natick, 2009.
15. Mollazade, K., Omid, M. and Arefi, A., 2012. Comparing Data Mining Classifiers for Grading Raisins Based on Visual Features. *Comput. Electron. Agr.*, **84:** 124–131.
16. Momenzadeh, L., Zomorodian, A. and Mowla, D. 2012.Applying Artificial Neural Network for Drying Time Prediction of Green Pea in a Microwave Assisted Fluidized Bed Dryer. *J. Agr. Sci. Tech.,* **14:** 513-522.
17. Omid, M., Khojastehnazhand M. and Tabatabaeefar, A. 2010a. Estimating Volume and Mass Citrus Fruits by Image Processing Technique. *J. Food Eng.*, **100**: 315–321.
18. Omid, M., Mahmoudi A. and Omid, M. H. 2010b. Development Pistachio Sorting System Using Principal Component Analysis (PCA) Assisted Artificial Neural Network (ANN) Impact Acoustics. *Expert Syst. Appl.,* **37:** 7205–7212.
19. Otsu, N. 1979. A Threshold Selection Method from Gray-level Histograms. *IEEE Transactions Systems, Man, Cybernetics,* **9**: 62–66.
20. Pedreschi, F., León, J., Mery, D. and Moyano, P. 2006. Development of a Computer Vision System to Measure the Color Potato Chips. *Food Res. Int.,* **39**: 1092–1098.
21. Polder, G., van der Heijden, G.W. A. M. and Young, I. T. 2003. Tomato Sorting Using Independent Component Analysis on Spectral Images. *Real-Time Imaging*, **9**: 253–259.
22. Taghadomi-Saberi, S., Omid, M., Emam-Djomeh, Z. and Ahmadi, H. 2014. Evaluating the Potential of Artificial Neural Network and Neuro-fuzzy Techniques for Estimating Antioxidant Activity and Anthocyanin Content of Sweet Cherry during Ripening by Using Image Processing. *J. Sci. Food Agric.,* **94:** 95–101.
23. Serrano, M., Guillean, F., Martı´nez-Romero, D., Castillo, S. and Valero, D. 2005. Chemical Constituents and Antioxidant Activity of Sweet Cherry at Different Ripening Stages. *J. Agric. Food Chem.,* **53:** 2741-2745.
24. Serrano, M., Guillean, F., Martı´nez-Romero, D., Castillo, S. and Valero, D. 2005. Chemical Constituents and Antioxidant Activity of Sweet Cherry at Different Ripening Stages. *J. Agr. Food Chem.,* **53:** 2741-2745.
25. Taghadomi-Saberi, S., Omid, M., Emam-Djomeh, Z. and Ahmadi, H. 2013. Estimation of Sweet Cherry Antioxidant Activity and Anthocyanin Content during Ripening by Artificial Neural Network–assisted Image Processing Technique. *Int. J. Food Sci. Technol.*, **48**: 735–741.
26. Unay, D., Gosselin, B., Kleynen, O., Leemans, V., Destain, M. F. and Debeir, O. 2011. Automatic Grading Bi-colored Spples by Multispectral Machine Vision. *Comput. Electron. Agr.,* **75:** 204–212.
27. Valadez-Blanco, R., Virdi, I. S., Balke, S. T. and Diosady, L. L. 2007. In-line Color Monitoring during Food Extrusion: Sensitivity and Correlation with Product Color. *Food Res. Int.,* **40**: 1129–1139.
28. Venora, G., Grillo, O. and Saccone, R. 2009. Quality Assessment of Durum Wheat Storage Centres in Sicily: Evaluation Vitreous, Starchy and Shrunken Kernels Using an Image Analysis System. *J. Cereal Sci.,* **49:** 429–440.
29. Wu, J. and Chan, J. 2009. Faulted Gear Identification of a Rotating Machinery Based on Wavelet Transform and Artificial Neural Network. *Expert Syst. Appl.*, **36**: 8862-8875.
30. Yam, K. L., and Papadakis, S. E. 2004. A Simple Digital Imaging Method for Measuring and Analyzing Color Food Surfaces. *J. Food Eng.*, **61**: 137–142.

31. Yoshida, K., Ito, D., Shinkai, Y. and Kondo, T., 2008. Change Color and Components in Sepalschameleon Hydrangea during Maturation and Senescence. *Phytochem.,* **69**: 3159–3165.

32. Zhou, T., Harrison, A. D., McKellar, R., Young, J. C., Odumeru J., Piyasena, P., Lu, X., Mercer, D. G. and Karr, S. 2004. Determination Acceptability and Shelf Life Ready-to-use Lettuce by Digital Image Analysis. *Food Res. Int.*, **37:** 875–881.

تعیین پارامترهای رنگی گیلاس طی مراحل رسیدگی با استفاده از تکنیک شبکه های عصبی مصنوعی و پردازش تصویر

س. تقدمی صابری، م. امید، ز. امام جمعه، خ. فرجی مهیاری

چکیده

بین کلاس های مختلف ویژگی های فیزیکی محصولات غذایی، رنگ مهم ترین ویژگی بصری برای ارزیابی کیفیت است. مصرف کنندگان تمایل دارند که رنگ را به کیفیت ارتباط دهند؛ زیرا رنگ با ارزیابی های کیفی فیزیکی، شیمیایی و حسی محصولات غذایی همبستگی خوبی دارد. در این مطالعه روشی ارزان قیمت برای پیش بینی پارامترهای رنگی گیلاس با استفاده از تکنیک های پردازش تصویر و شبکه عصبی مصنوعی ارائه شده است. چیدمان استفاده شده در این مطالعه شامل یک دوربین CCD برای تصویربرداری و نرم افزار متلب برای مدلسازی شبکه عصبی و پردازش تصویر بود. به منظور ارزیابی این روش، تغییرات رنگ گیلاس طی مراحل رسیدگی مورد بررسی قرار گرفت. پس از طراحی، آموزش و تولید شبکه های عصبی متعددی با استفاده از الگوریتم لونبرگ- مارکوارت، در نهایت شبکه ای با توپولوژی ۳-۱۱-۱۴-۷ به عنوان شبکه بهینه انتخاب شد. این شبکه دارای ضریب تبین ۰/۹۹۹۹ برای مقادیر *L، *a و *b به دست آمده از کرومامتر و سامانه ماشین بینایی مورد بررسی بود. پارامترهای *L و *b طی مراحل رسیدگی روند کاهشی نشان دادند در حالی که پارامتر *a در ابتدا افزایش و سپس کاهش می یافت. ارزیابی مقادیر *L، *a و *b امکان استفاده قابل اطمینان از این سامانه را برای تخمین مقادیر رنگی محصولات غذایی با قیمتی پایین در مقایسه با کرومامتر نشان داد.